Caving 2026 – A van As, D Cumming-Potvin & J Wesseloo (eds)

doi:10.36487/ACG_repo/2645_21

The role of rock mass modulus and structure on cave propagation behaviour

Bre-Anne Sainsbury [a,*], David Sainsbury [b]

[a] *School of Engineering, Deakin University, Australia*

[b] *Geotechnica Pty Ltd, Australia*

Abstract

Caveability is commonly assessed using strength-based approaches. However, field observations show that cave propagation often deviates from these predictions, even when sophisticated numerical predictions are completed. This paper examines the role of rock mass modulus and damage evolution in controlling cave behaviour under excavation-induced unloading stress paths. Conceptual modelling demonstrates that for identical strength parameters, variations in rock mass modulus produce order of magnitude differences in prediction of cave height, propagation rate and tonnes extracted. Stress path analysis shows that the key difference between rock mass modulus cases is therefore not the stress path itself, but how far that path progresses towards failure. In higher stiffness rock masses, damage remains distributed and propagation is constrained, whereas lower stiffness conditions promote localisation and sustained growth and progress further towards failure. Geological structure enhances cave propagation only when intersected and when the stiffness regime permits damage localisation. The results demonstrate that in some cases, cave propagation is governed by stiffness-controlled damage evolution rather than strength exceedance alone, and that rock mass modulus must be treated as a primary input parameter in caveability assessments. However, reliable estimation of modulus remains highly uncertain, as commonly used empirical relationships can produce values that differ by an order of magnitude or more for the same rock mass. This variability introduces significant uncertainty into design and reinforces the need to more routinely characterise rock mass modulus through in situ monitoring and back-analysis.

Keywords: *caving, cave propagation, cave initiation, crack damage criterion, rock mass modulus, structure*

1 Introduction

Caveability assessments and cave growth predictions are central to the design, scheduling, and risk management of cave mining methods and are commonly derived from strength and stress-based criteria. At the pre-feasibility and feasibility stages, it is generally accepted that these predictions are subject to uncertainty arising from limited geological information, variability in rock mass properties, and simplifying assumptions inherent in underground excavation design. As such, some divergence between predicted and observed cave behaviour is accepted as undercutting and production draw progresses, however, certainty in cave propagation predictions should improve as the local geomechanical understanding improves.

Historically, numerous mines have experienced cave propagation behaviour that either significantly exceeded expectations or failed to develop altogether despite apparently favourable strength and stress conditions predicted during the study stages (Table 1). In many cases, these outcomes have occurred even where detailed geotechnical characterisation, calibration, and sophisticated modelling were undertaken. The recurrence of such behaviour across different cave geometries, stress environments, and rock mass types indicates that the divergence cannot be explained solely by uncertainty in input parameters or model

* Corresponding author. Email address: breanne.sainsbury@deakin.edu.au

resolution. Instead, it suggests a more fundamental limitation in the criteria used to interpret rock mass caveability and propagation behaviour.

Table 1 Documented divergence between predicted and observed cave behaviour

Mine	Observed behaviour	Reference
Andina Mine	Very high in situ stresses and competent rock led to complex, and sometimes unstable cave behaviour, including difficult cave propagation, stress-driven damage, and seismic response.	(Sougarret et al. 2004)
Argyle Mine	Propagation was difficult, non-uniform, and required significant preconditioning. Less than 60% of the original mining reserve was recovered.	(Stegman et al. 2018)
Cadia East PC1	Cave initiation occurred as expected, but upward propagation stalled against a very competent, high-stiffness cap rock, before later reinitiating and accelerating once preconditioning from the surface occurred.	(Sainsbury et al. 2018)
Chuquicamata	Propagation was more complex and hazardous than expected due to higher in situ stresses, modulus and strong structural control. Conditions resulted in seismic damage, non-uniform propagation, and the need for preconditioning.	(Constanzo et al. 2020)
El Teniente Block 22	Cave behaviour characterised by a slow initial cave propagation rate, a tendency for a flat cave back. Arrest was sooner than expected.	(Hekmatnejad et al. 2025)
Grasberg Deep Ore Zone (DOZ)	Propagation occurred under extremely high stress conditions but was highly heterogeneous, with rapid growth along structurally weakened, low-stiffness domains and delayed or arrested propagation in more competent rock.	(Campbell et al. 2020)
Northparkes E26	Cave initiation occurred locally near the undercut, propagation was delayed and spatially uneven and large volumes of rock remained load bearing for longer than expected requiring additional hydraulic fracturing preconditioning.	(Van As & Jeffrey 2000)
Northparkes E48	Actual propagation rates significantly exceeded expectations with surface connection achieved early. However, estimated up to 4.8 Mt of reserves remained outside the initial cave volume on the north and south boundaries.	(Snyman et al. 2016)
Palabora block cave	Cave propagation accelerated rapidly once initiated (initiation delayed). Cave height growth exceeded expectations. Extensive surface subsidence developed earlier and over a wider area than predicted.	(Sainsbury et al. 2008, 2016; Woo et al. 2012)
Ridgeway Deeps	Cave propagation progressed largely as expected within the sedimentary units; however, in the volcanic domain, propagation was problematic and a stable haunch developed.	(Lett 2024)
Ridgeway sublevel cave	Propagation as locally accelerated where a major fault was intersected.	(Brunton 2009)

One contributing factor for such divergence in behaviour is that cave propagation is commonly assessed using static representations of rock mass strength compared against in situ or induced stress (Laubscher 2010, 1994; Mathews 1980; Mawdesley et al. 2001). These static stress analyses implicitly assume that increasing σ_1 drives rock mass failure. In reality, rock mass strength is stress path dependent. For example, under increasing σ_1, strength may increase, decrease, or remain unchanged depending on the evolution of confinement (σ_3) as illustrated in Figure 1. In general, stress distribution around an excavation is associated with a progressive reduction in σ_3, representing an unloading stress path as confinement is removed.

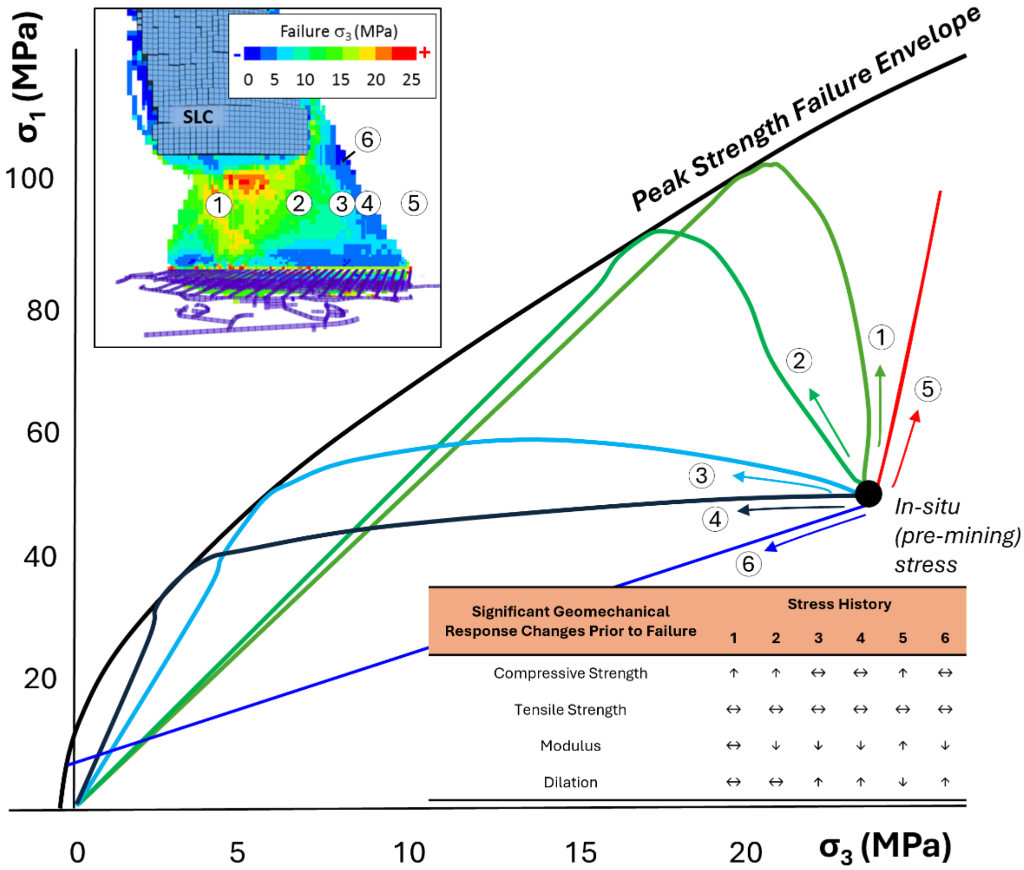

Significant Geomechanical Response Changes Prior to Failure	Stress History 1	2	3	4	5	6
Compressive Strength	↑	↑	↔	↔	↑	↔
Tensile Strength	↔	↔	↔	↔	↔	↔
Modulus	↔	↓	↓	↓	↑	↓
Dilation	↔	↔	↑	↑	↓	↑

Figure 1 Stress paths around a propagating cave in confined high stress conditions

Strength-based cave prediction methods collapse fundamentally different stress paths into a single measure of proximity to failure - an assumption that is too broad for the various stress paths that occur around a propagating cave (Figure 1). Because σ_1 at failure depends on σ_3, peak strength cannot be treated as a fixed reference point during the caving process. Experimental studies demonstrate that rock response under unloading stress paths differs fundamentally from that observed under loading stress paths (Rooz & Sainsbury 2026a, 2026b). Unloading is characterised by progressive modulus degradation and increasing deformation, even when peak compressive strength is not mobilised. Part of this stiffness reduction reflects the loss of confinement in the elastic response (Sainsbury & Rooz 2025). However, this does not explain the permanent plastic changes to the modulus that have been measured in the laboratory (Rooz & Sainsbury 2026a, 2026b). These permanent changes suggest a more mechanistic framework is required that is able to consider strength along with damage evolution during unloading (reduction in σ_3) that accompanies cave propagation.

2 Role of crack damage in cave propagation

The crack damage criterion (CDC) framework – first introduced by Martin (1993) – provides a mechanistic basis for interpreting cave propagation under excavation-driven unloading stress paths. The CDC framework separates rock response into 2 key stages: failure initiation, associated with the onset of distributed microcracking (crack initiation CI), and failure propagation (crack damage CD), governed by the evolution and coalescence of damage behaviour (Figure 2a), both of which are mapped to the conceptual model of caving and presented in Figure 2b. For rock, the CI threshold broadly correlates with the onset of seismicity (the seismogenic zone) surrounding a propagating cave, while the CD threshold corresponds to the yield (aseismic) zone. In this respect, it is important to observe that a yielded/damaged rock mass does not necessarily imply a mobilised rock mass. Typical CI and CD values for rocks are summarised in Table 2.

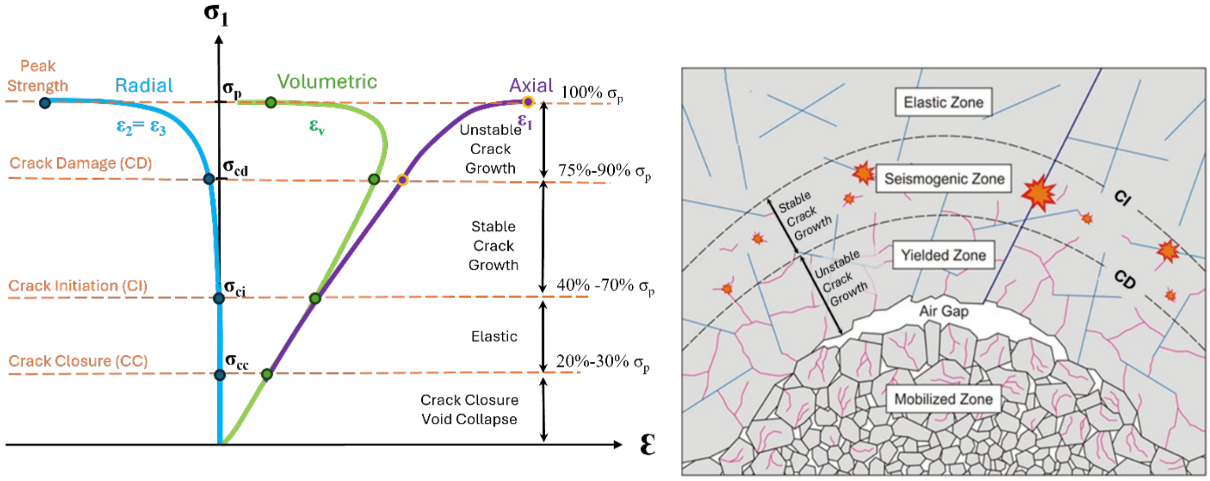

(a) (b)

Figure 2 (a) Crack damage criterion modified after Rooz & Sainsbury (2025b); (b) Regions of a propagating cave defined by crack damage thresholds modified after Sainsbury (2012)

Table 2 Rock type versus typical crack damage criterion threshold values

Rock type	**(% max σ_1 at failure)**				**Reference**
	Crack initiation (CI) **(Stable crack growth)**		**Crack damage (CD)** **(Unstable crack growth)**		
Kimberlite	Early damage,	40–55	Short damage phase,	75–90	(Tyler & Godden 2008)
Granite	early stiffness loss,	40	brittle failure,	75	(Rooz & Sainsbury 2025b)
Volcanics	early initiation ↓	45–60	limited propagation ↓	75–90	(Heap & Faulkner 2008)
Limestone	↓	50–60	Prolonged damage evolution,	80–90	(Eberhardt et al. 1999)
Sandstone	Delayed damage, stiffer response,	60	progressive stiffness loss, more	80	(Rooz & Sainsbury 2026b)
Carbonatite	delayed initiation	60–70	sustained propagation	80–90	(Mas Ivars et al. 2011)

The wide range in reported CDC thresholds, approximately 40–70% of σ_1 at failure for CI and 75–90% for CD, provides a mechanical explanation for the variability observed in caving responses that is not associated with peak strength. Rocks with low CI and CD thresholds tend to initiate damage and modulus degradation at relatively low stress levels, leading to the development of extensive seismogenic and yielded zones during early cave propagation. In contrast, rocks with higher thresholds may exhibit limited or negligible seismogenic or yield zones despite continued cave advance. Importantly these differences highlight that cave initiation and cave propagation are governed by different aspects of rock behaviour. CI primarily controls when distributed microcracking begins and therefore the likelihood of cave initiation. However, propagation behaviour depends on the damage evolution window between CI and CD. Lithologies characterised by a narrow CI–CD interval and rapid modulus collapse are prone to abrupt instability and rapid cave advance once damage localises, whereas rocks with a wider CI–CD interval tend to accommodate distributed deformation and progressive modulus degradation.

When interpreted alongside the documented case histories summarised in Table 1, these differences help explain why caves with comparable strength classifications have exhibited markedly different in situ responses. Operations such as Andina, Chuquicamata, and El Teniente Block 22 are hosted in strong porphyry systems (andesite–diorite–granodiorite). These rocks exhibit relatively low CI with a wide CI–CD interval (Table 2) resulting in early damage initiation but delayed localisation. This response is typical of flat cave backs, propagation arrest, and a strong seismic response. Examples such as Palabora Block Cave, hosted in carbonatite (Table 2) reflect a rock mass that has a high CI and narrow CI–CD interval. In these cases, once damage initiates it rapidly localises leading to abrupt cave propagation. Northparkes E26 hosted in a porphyry Cu-Au system exhibited constrained propagation with periods of stall, consistent with a stress path that initiated damage but did not readily progress toward localisation (i.e. limited progression from CI toward CD) (Reyes-Montes et al. 2016). Microseismic imaging and modulus-based modelling showed that fracturing initiated and evolved over a wide stress range ahead of the cave back, consistent with a wide CI–CD interval. Together, these cases demonstrate that cave propagation is governed not by strength classification alone, but by the position and separation of CI and CD for each rock type. The separation between CI and CD is fundamentally controlled by the cave system stiffness, implying that modulus becomes a controlling parameter for propagation.

3 Role of modulus in cave propagation

A compilation of empirical equations has been applied to a representative cave mine host rock mass (Table 3) to generate a range of rock mass modulus (E_{rm}) estimates (Figure 3). For an identical rock mass description, estimated values of E_{rm} vary by an order of magnitude. Furthermore, for the universally adopted Hoek & Diederichs (2006) formulation incorporating E_i, additional variability arises depending on whether a secant (E_{sec50}) or tangent (E_{tan50}) value for the E_i is selected.

Table 3 Rock mass strength parameters

Intact				Rock mass	
σ_{ci} (MPa)	m_i	E_{sec50} (GPa)	E_{tan50} (GPa)	Geological strength index	σ_{cm} (MPa)
100	20	68.1	84.9	60	10.7

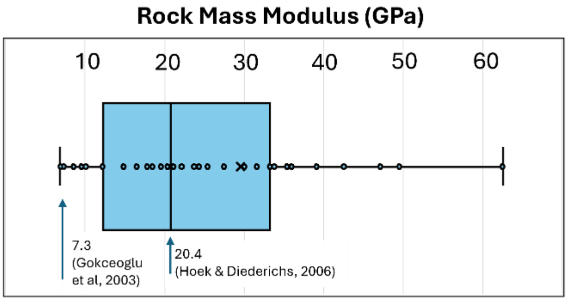

Figure 3 Empirical rock mass modulus estimates

To illustrate the impact of variability of E_{rm} estimates on cave propagation behaviour, conceptual numerical simulations were undertaken for a representative orebody at 580 m depth under a 1.7:1.0 horizontal-to-vertical stress regime. The same conceptual model has been used to consider the impact of peak strength, softening rate, m_i, stress/depth, bulking behaviour and draw strategy on caving behaviour and are documented in Sainsbury (2010). The conceptual modelling approach incorporates several simplifying assumptions. For example, the rock mass is represented using an equivalent continuum strain softening, bilinear, Mohr–Coulomb constitutive model, with rock mass properties derived from equivalent Hoek–Brown parameter conversions. Post-peak behaviour and brittleness are inferred from assumed relationships with geological strength index and model zone size and density, modulus, and dilation evolve automatically with volumetric strain to maintain mass conservation (Sainsbury, 2012). Production draw is simulated using simplified pseudo-static velocity boundary conditions and variability in production was simplified to an assumed +/-10% difference between drawpoints across the fixed footprint.

In the case presented herein, the rock mass strength parameters were held constant (Table 3), while the E_{rm} was varied. A lower-bound estimate of E_{rm} at 7.3 GPa based on Gokceoglu et al. (2003) and a mean E_{rm} estimate of 20.4 GPa based on the simplified relationship of Hoek & Diederichs (2006) were selected for comparison along with E_{rm} estimates of 35.4 GPa and 44.1 GPa derived from Hoek & Diederichs (2006) incorporating E_{sec50} and E_{tan50} (Table 3) as the E_i values respectively. The resulting propagation response following identical Height of Draw (HOD) simulation up to 100 m vertical draw is summarised in Figure 4. Rock mass bulking behaviour and production draw has been simulated based on the relations described in Sainsbury (2012, 2019).

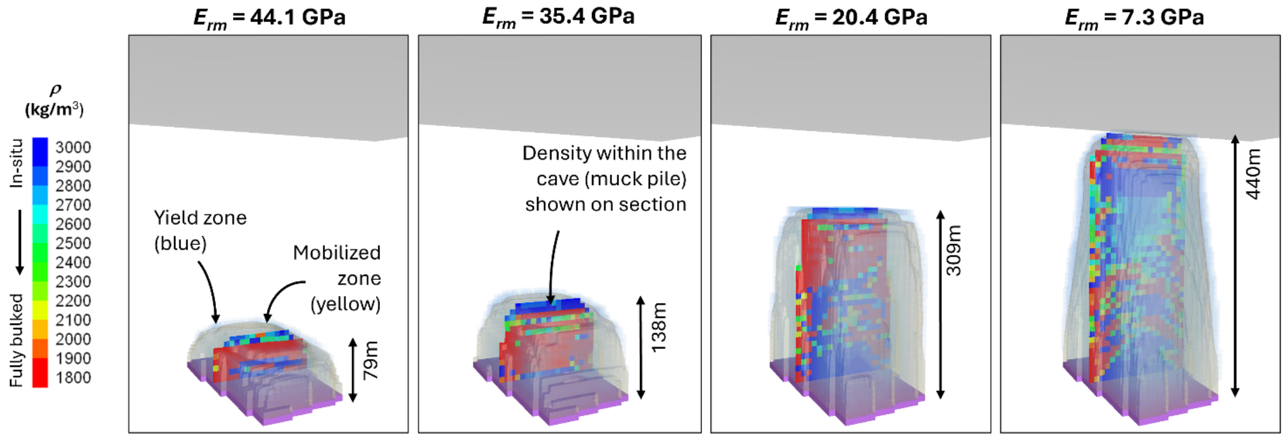

Figure 4 Evolution of cave geometry and density distribution after 100 m of simulated draw

Although identical peak strength parameters were adopted in all simulations, the propagation response varies significantly with the E_{rm} value simulated. A summary of the results of cave height, propagation rate and tonnes extracted are provided in Figure 5.

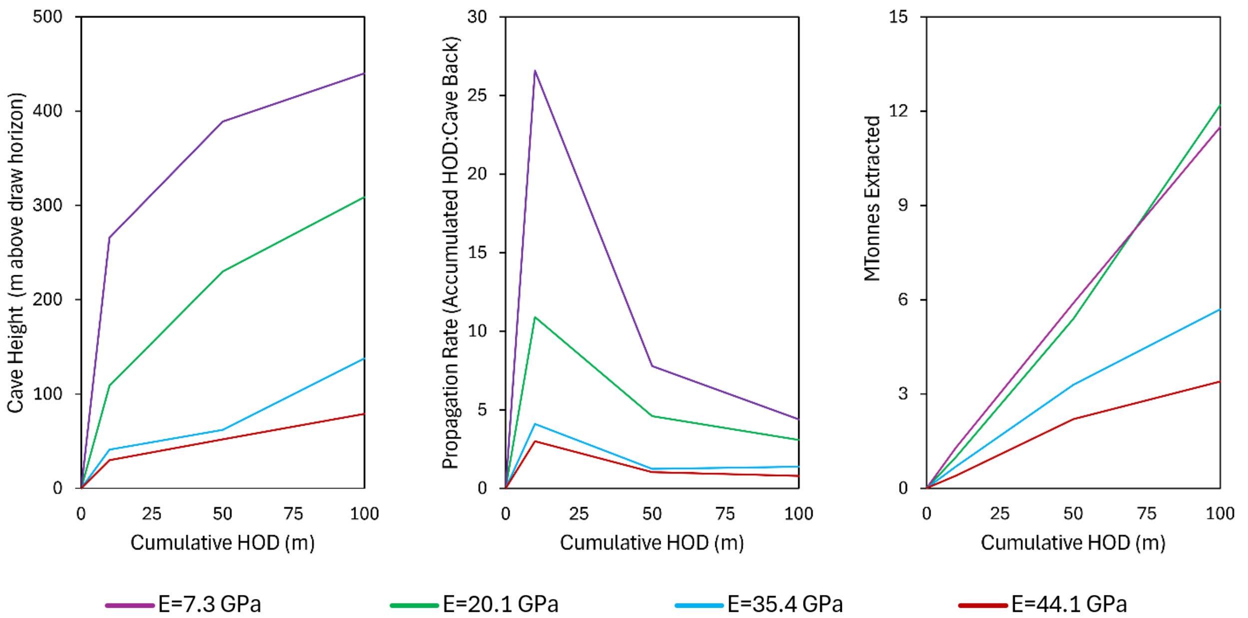

Figure 5 Effect of E_{rm} on cave propagation response

Variation in E_{rm} produces large differences in cave height, propagation rate and tonnes extracted under identical strength conditions, with lower modulus rock masses exhibiting rapid early propagation and higher modulus rock masses showing constrained or delayed growth. At a HOD of 100 m, the E_{rm} 7.3 GPa model produces cave heights of approximately 440 m, whereas the E_{rm} 44.1 GPa model is limited to 70 m. Similar differences are evident at early draw (height of draw 10 m), where propagation in the E_{rm} 7.3 GPa case already exceeds 250 m compared with less than 30 m in the E_{rm} 44.1 GPa case. These results indicate that cave propagation behaviour is established very early in the production sequence modelled and is not governed primarily by strength, but by the ability of the rock mass to accommodate deformation. The intermediate E_{rm} values simulated exhibit transitional behaviour, with propagation reducing progressively between E_{rm} 20.4 GPa and E_{rm} 35.4 GPa rather than shifting abruptly between propagating and stalled states. This continuous reduction in cave height and mobilisation with increasing E_{rm} values indicates that propagation capacity is influenced by deformation and damage evolution rather than by a discrete peak strength threshold. As shown in Figure 5, early differences in propagation rate persist throughout production, leading to sustained divergence in cave height and tonnes extracted.

Notably, the extracted production tonnes in the E_{rm} 20.4 GPa model are comparable to those of the E_{rm} 7.3 GPa simulation, despite a difference in cave back height exceeding 100 m. Inspection of the density distribution within the cave column (Figure 4) shows that the E_{rm} 7.3 GPa case exhibits reduced bulking, requiring greater vertical propagation to extract equivalent tonnes. In contrast, the intermediate case (E_{rm} 20.4 GPa) promotes increased bulking resulting in a shorter vertical extent of the cave for the same tonnes extracted. At higher modulus values (E_{rm} 35.4–44.1 GPa), this trend does not continue. Although bulking remains elevated, cave propagation becomes increasingly constrained, with limited upward growth and reduced overall tonnes extracted. In these cases, the rock mass retains sufficient stiffness to inhibit damage localisation, preventing sustained propagation despite ongoing draw. Together, these results indicate the presence of a non-linear response, where an intermediate stiffness regime provides the most efficient mobilisation. Low modulus conditions favour propagation but with limited bulking, while high modulus conditions suppress propagation altogether. The intermediate regime represents a balance between damage accumulation, fragmentation and stress redistribution, suggesting that cave performance is maximised within a bounded stiffness range, rather than improving monotonically with decreasing modulus.

To further examine differences in propagation behaviour, the stress path evolution above the draw horizon for each E_{rm} case is shown in Figure 6. Despite the significant differences in cave propagation behaviour observed across the rock mass modulus cases, the corresponding stress path responses above the draw horizon are broadly similar for all models. All models follow a consistent unloading trajectory, characterised by decreasing σ_3 with limited increase in σ_1, indicating that failure in many cases of cave propagation is driven by confinement loss rather than increasing σ_1 stress. This presents a fundamental inconsistency: if cave propagation were governed primarily by stress conditions or proximity to peak strength, similar stress paths would be expected to produce comparable propagation behaviour. However, the modelling results clearly demonstrate that this is not the case, with identical stress path trajectories resulting in either rapid cave growth or early arrest. This indicates that an additional mechanism is required to explain how the rock mass responds to the same unloading conditions.

The key difference between the E_{rm} cases is therefore not the stress path itself, but how far that path progresses towards failure. In lower E_{rm} conditions, unloading is accompanied by sufficient deformation to enable continued damage accumulation and upward propagation. In contrast, higher E_{rm} cases arrest earlier along the same unloading path, with damage remaining distributed and failing to localise. This is highlighted by the stalled cave conditions simulated in the E_{rm} 34.5 GPa and 44.1 GPa models above 370 m height, and E_{rm} 20.4 GPa case above 470 m height (Figure 6).

These stress path responses, clearly demonstrate that cave propagation in this scenario is governed by the stiffness-controlled response of the system to unloading rather than by different stress paths themselves. Identical stress paths can therefore result in either sustained propagation or early arrest depending on whether damage evolution can progress toward localisation (i.e. move from CI toward CD). However, the stress path alone does not determine whether this transition occurs. Instead, progression through the CI–CD interval is controlled by the capacity of the rock mass to deform under an unloading stress path, which is governed by rock mass modulus. In lower rock mass modulus conditions, deformation is readily accommodated, enabling progressive damage accumulation, stiffness degradation, and eventual localisation of failure. In contrast, increasing rock mass modulus progressively limits the capacity for deformation under unloading, restricting damage accumulation and suppressing localisation. As a result, although CI may be reached, the system is unable to advance toward CD, and propagation becomes constrained or stalls. The transition between these behaviours is strongly non-linear. Increasing rock mass modulus progressively limits the capacity for deformation under unloading, restricting damage accumulation and suppressing localisation. Beyond approximately E_{rm} 35 GPa in this scenario, this transition is effectively inhibited and propagation becomes strongly constrained.

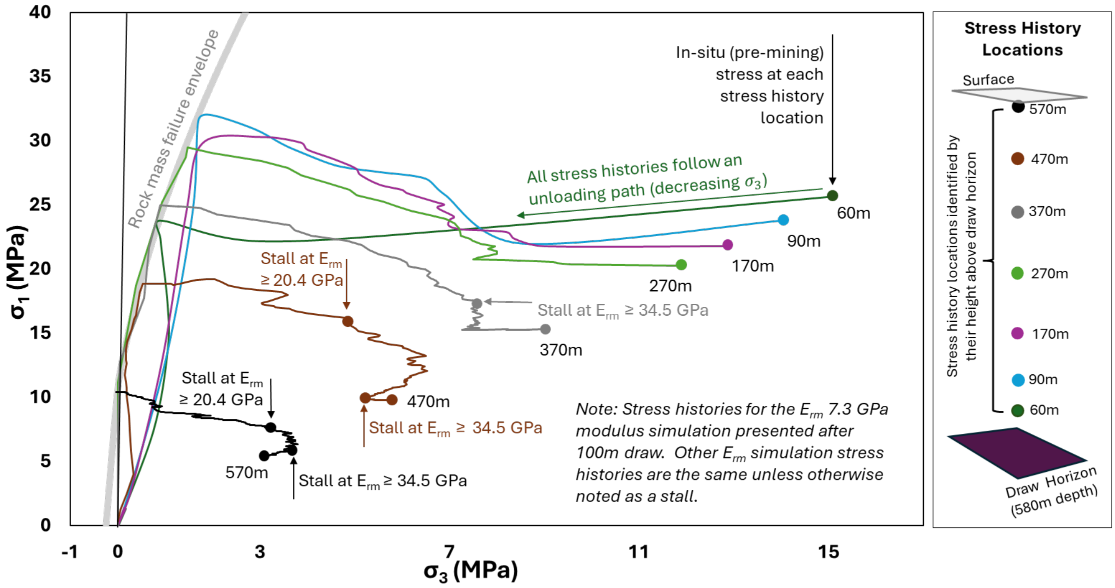

Figure 6 Stress path evolution for varying E_{rm} models during 100 m of simulated production draw

Mischaracterisation of E_{rm} therefore introduces significant uncertainty into design and forecasting, reinforcing the need to treat modulus as a primary parameter alongside strength and stress when conducting caving analyses. Peak strength alone is insufficient to assess caveability, and the strength at failure is not uniformly mobilised throughout the cave. Instead, cave propagation is governed by the interaction between rock mass modulus, stress path evolution under unloading, and the capacity for damage to accumulate and localise. At the present time, the reliable constraint of E_{rm} cannot be achieved through empirical relationships alone and must be derived from the observed response of the rock mass. Methods for observing E_{rm} can broadly be divided into direct and indirect approaches. Direct measurement methods involve in situ testing and are generally considered the most reliable techniques. Methods include flat jack tests, dilatometer tests, and plate loading/jacking tests. These methods directly measure deformation response under applied loading. However, they test only a relatively small rock volume and can only be applied in areas where direct access is possible. Indirect methods estimate modulus from geophysical or other large-scale observations. Common approaches include seismic testing (cross-hole, downhole, refraction, tomography, microseismic) which is non-invasive and can assess larger rock volumes, but they require detailed geological interpretation and specialists to interpret the results. As such, in practice, many projects ultimately rely on numerical back-analysis to constrain E_{rm}. A numerical approach compares modelled responses with observed in situ behaviour, requiring both stress (force) and displacement (strain) data to calibrate and bracket likely values. These in situ stress and strain responses are best measured over time within each geotechnical domain and key mining area, including the extraction level, undercut level, cave column, and abutment zones. By iteratively adjusting E_{rm} within numerical models until predicted deformations and stress redistributions align with field responses, a representative E_{rm} values can be back-calculated rather than assumed.

4 Role of structure in cave propagation

For the conceptual cave model, a vertical large-scale fault structure was introduced at the boundary of the extraction horizon (Figure 7). The fault has been simulated as a zone joint (ITASCA 2025) with stiffness of 1e10 KN/m, friction (ϕ) of 25° and cohesion and tension of 10 kPa. For each E_{rm} case (7.3, 20.1, 35.4 and 44.1 GPa) draw was re-simulated up to 100 m height to assess the impact of the simulated structure on propagation behaviour. Model results are provided in Figure 7.

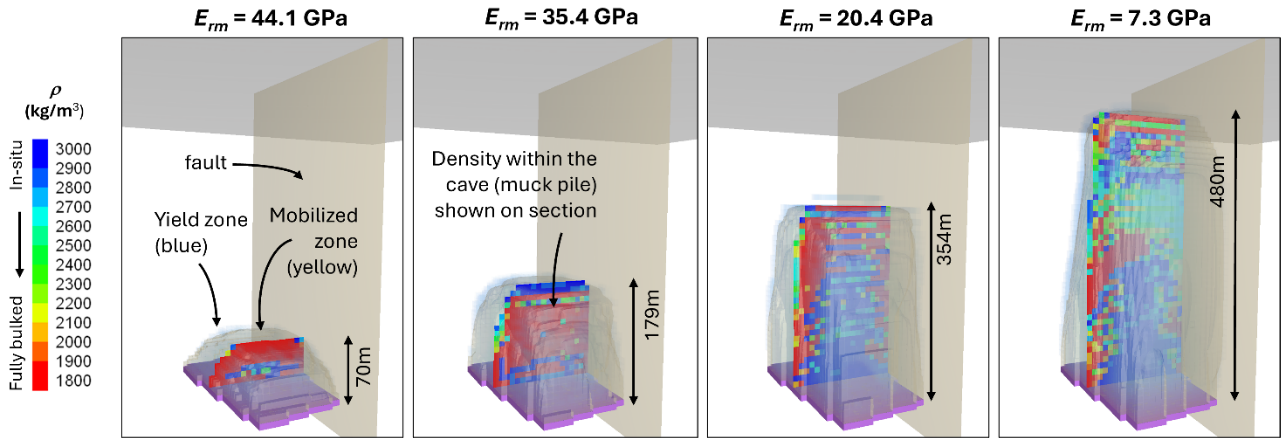

Figure 7 Evolution of cave geometry and density (ρ) distribution with structure for each E_{rm} value simulated

It is important to note that the structural analysis presented herein is conceptual in nature and incorporates several simplifying assumptions. Only a single vertical structure orientation and geometry is considered, represented as a planar, continuous and perfectly persistent feature with constant mechanical properties along its extent represented by a Mohr–Coulomb constitutive model. Variability in structural persistence, roughness, infill and orientation were not considered, nor was the influence of more complex discrete fracture networks. As such, the results are intended to demonstrate a conceptual interaction between structure, modulus and damage localisation, rather than provide any site-specific predictions of structurally controlled cave propagation. Nevertheless, the model results in this case show that the influence of structure on cave propagation is strongly dependent on the modulus of the rock mass. A comparison of the model responses with the structure are compared to the to their respective homogenous cases and is presented in Table 4.

Table 4 Impact of simulated structure on cave propagation response for each E_{rm} case

E_{rm} (GPa)	HOD (m) 10	50	100	Simulated response	Compared to homogeneous response at 100 m draw
7.3[1]	279, *27.9*	445, *8.9*	480, *4.8*	Cave height (m), *Propagation rate*	+40 m, *+0.4*
	1.3	6.3	13.0	MTonnes mobilised (muckpile)	+1.5
20.4[2]	145, *14.5*	279, *5.6*	354, *3.5*	Cave height (m), *Propagation rate*	+45 m, *+0.4*
	1.0	5.8	12.6	MTonnes mobilised (muckpile)	+0.4
35.4[3]	44, *4.4*	114, *2.3*	179, *1.8*	Cave height (m), *Propagation rate*	+41 m, *+0.4*
	0.7	3.8	8.0	MTonnes mobilised (muckpile)	+2.3
44.1[4]	29, *2.9*	51, *1.0*	70, *0.7*	Cave height (m), *Propagation rate*	-9 m, *-0.2*
	0.7	2.3	3.2	MTonnes mobilised (muckpile)	-, *-0.2*

[1] (Gokceoglu et al. 2003); [2] (Hoek & Diederichs 2006) Simplified; [3] (Hoek & Diederichs 2006) $\mathrm{E_{sec50}}$; [4] (Hoek & Diederichs 2006) $\mathrm{E_{tan50}}$

The modelling results demonstrate that structural discontinuities enhance propagation only when they are intersected and when sufficient deformation occurs to enable damage localisation. In low modulus conditions (E_{rm} 7.3 GPa), where the rock mass readily accumulates damage under unloading, the inclusion of structure significantly increases cave height, propagation rate and extracted tonnes. Once intersected, the structure provides a preferential pathway for damage connectivity, accelerating localisation and enabling more efficient upward propagation. At intermediate modulus values (E_{rm} 20.4-35.4 GPa), the response reflects a transitional regime. Structure continues to enhance propagation; however, its influence is more variable and dependent on the extent and timing of interaction with the structure surface. In these cases, structure assists the transition from distributed damage toward localisation but does not fully overcome the underlying stiffness constraint. In contrast, under high modulus conditions (E_{rm} 44.1 GPa), the inclusion of structure produces negligible change in propagation behaviour. Although structural discontinuities are present, limited deformation prevents sufficient damage accumulation and localisation. As a result, propagation remains constrained despite continued draw. This demonstrates that structure alone cannot drive propagation unless it is intersected.

Comparison of cave height and mobilised tonnes (Table 4) indicates that the influence of structure is not limited to propagation extent but also affects fragmentation and bulking behaviour within the cave column. In cases where structure enhances propagation, increases in cave height are not always matched by proportional increases in extracted tonnage, suggesting that deformation is redistributed along structural surfaces rather than resulting in localised volumetric expansion. This implies reduced bulking efficiency within structurally controlled propagation regimes, with deformation accommodated through shear and displacement along discontinuities. These results demonstrate that structure does not always act as an independent driver of cave propagation, but as a modifier of stiffness-controlled system behaviour. Structural features act as agents of change only when intersected and when the stiffness regime permits damage localisation (stress path moves from CI towards CD). Where these conditions are met, structure enhances connectivity and accelerates propagation; where they are not, structure has little influence and propagation remains constrained. These results also demonstrate that cave propagation must be assessed with the incorporation of large-scale structure. While strength defines the onset of damage, sustained propagation is governed by stiffness-controlled damage evolution under unloading, with geological structure modifying where and how that damage localises.

Collectively, these findings have several important implications for caveability assessment and cave mine design. From a practical perspective, the results demonstrate that caveability assessments should not rely solely on peak strength or empirical caveability classifications. Instead, rock mass modulus should be treated as a primary sensitivity or calibration parameter during numerical modelling and observational back-analysis. Practitioners should evaluate multiple plausible modulus scenarios during project studies and progressively constrain these values using in situ monitoring throughout cave development and production. The CDC framework which may be quantified at the rock mass scale through microseismic monitoring or synthetic rock mass studies provides a practical basis for interpreting whether cave growth is likely to remain distributed, localise, accelerate or arrest under unloading stress paths. The study also demonstrates that geological structure should not automatically be assumed to enhance cave growth, as its influence depends on both structural intersection and the stiffness-controlled capacity of the system to localise damage.

5 Conclusion

Cave propagation is not governed by strength exceedance alone. Conceptual modelling demonstrates that in some cases rock mass modulus exerts a first-order control on propagation behaviour and that structural discontinuities enhance propagation only when intersected and when the system stiffness permits damage localisation. These results (although limited in scope) demonstrate that strength-based caveability approaches are insufficient in many cases to rigorously resolve cave propagation behaviour. Mischaracterisation of E_{rm} therefore introduces significant uncertainty into design and forecasting, reinforcing the need to treat rock mass modulus as a primary parameter alongside strength and stress in caveability assessment. However, reliable estimation of modulus remains fundamentally challenging. As demonstrated in this study and widely reported in the literature, empirical relationships commonly produce values that differ by factors of 2 to 10 for the same rock mass, with no clear basis for selection or validation. This variability is not simply a matter of parameter scatter, but reflects the inherent limitations of empirical approaches, which cannot adequately capture the combined effects of structure, scale, stress level and damage evolution governing rock mass stiffness. As a result, modulus is routinely mischaracterised at the design stage, and these errors propagate directly into predictions of cave propagation, subsidence, seismicity and support demand. Consequently, reliance on empirical rock mass modulus estimates alone introduces significant uncertainty in design outcomes. Rock mass modulus must instead be constrained through an observational approach, integrating in situ monitoring with back-analysis of the evolving cave response to derive an effective system stiffness. Within and around a cave mine, it must also be acknowledged that rock mass modulus is not a fixed material constant, but an emergent property of stress path dependent damage evolution.

References

Brunton, I 2009, *The Impact of Blasting on Sublevel Caving Material Flow Behaviour and Recovery*, PhD thesis, University of Queensland, Brisbane.

Campbell, R, Mardiansyah, F, Banda, H, Tshisens, J, Griffiths, C & Beck, D 2020, 'Early experiences from the Grasberg block cave: A rock mechanics perspective', in R Castro, F Báez & K Suzuki (eds), *MassMin 2020: Proceedings of the Eighth International Conference & Exhibition on Mass Mining*, University of Chile, Santiago, pp. 115–126, https://doi.org/10.36487/ACG_repo/2063_03

Constanzo, HE, Guerra, PC & Barindelli, GA 2020, 'Observational rock mass damage model associated to caving advance of Chuquicamata Underground Mine', in R Castro, F Báez & K Suzuki (eds), *MassMin 2020: Proceedings of the Eighth International Conference & Exhibition on Mass Mining*, University of Chile, Santiago, pp. 910–921, https://doi.org/10.36487/ACG_repo/2063_65

Eberhardt, E, Stead, D & Stimpson, B 1999, 'Quantifying progressive pre-peak brittle fracture damage in rock during uniaxial compression', *International Journal of Rock Mechanics and Mining Sciences*, vol. 36, pp. 361–380, https://doi.org/10.1016/S0148-9062(99)00019-4

Gokceoglu, C, Sonmez, H & Kayabasi, A 2003, 'Predicting the deformation moduli of rock masses', *International Journal of Rock Mechanics and Mining Sciences*, vol. 40, pp. 701–710, https://doi.org/10.1016/S1365-1609(03)00062-5

Heap, MJ & Faulkner, DR 2008, 'Quantifying the evolution of static elastic properties as crystalline rock approaches failure', *International Journal of Rock Mechanics and Mining Sciences*, vol. 45, pp. 564–573, https://doi.org/10.1016/j.ijrmms.2007.07.018

Hekmatnejad, A, Manscilla, F, Schachter, P, Pan, P, Mohtarami, E, Pena, A, … Gonzales, R 2025, 'Enhancing production rates at El Teniente's black cave mine through optimizing HF hole distribution using discrete fracture network modeling and geostatistical simulation methods', *Rock Mechanics Bulletin*, vol. 4, article 100165, https://doi.org/10.1016/j.rockmb.2024.100165

Hoek, E & Diederichs, MS 2006, 'Empirical estimation of rock mass modulus', *International Journal of Rock Mechanics and Mining Sciences*, vol. 43, pp. 203–215, https://doi.org/10.1016/j.ijrmms.2005.06.005

ITASCA 2025, *FLAC3D 9.0 Fast Lagrangian Analysis of Continua in Three-Dimensions*, version 9.0, Minneapolis.

Laubscher, D 1994, 'Cave mining—the state of the art', *Journal of the South African Institute of Mining and Metallurgy*, pp. 279–293.

Laubscher, D 2010, *A Practical Manual on Block Caving*, 2nd edn, University of Queensland, Brisbane.

Lett, J 2024, 'Geotechnical lessons learnt during undercutting in deep caving at Cadia Operations', in P Andrieux & D Cumming-Potvin (eds), *Deep Mining 2024: Proceedings of the 10th International Conference on Deep and High Stress Mining*, Australian Centre for Geomechanics, Perth, pp. 109–136, https://doi.org/10.36487/ACG_repo/2465_02

Martin, C 1993, *The Strength of Massive Lac du Bonnet Granite Around Underground Openings*, PhD thesis, University of Manitoba, Winnipeg.

Mas Ivars, D, Pierce, ME, Darcel, C, Reyes-Montes, J, Potyondy, DO, Young, RP & Cundall, PA 2011, 'The synthetic rock mass approach for jointed rock mass modelling', *International Journal of Rock Mechanics and Mining Sciences*, vol. 48, pp. 219–244, https://doi.org/10.1016/j.ijrmms.2010.11.014

Mathews, K 1980, *Prediction of Stable Excavation Spans for Mining at Depths Below 1,000 Meters in Hard Rock*, viewed 23 January 2026, https://osdp-psdo.canada.ca/dp/en/search/metadata/NRCAN-GEOSCAN-1-331949

Mawdesley, C, Trueman, R & Whiten, W 2001, 'Extending the Mathews stability graph for open-stope design', *Transactions of the Institution of Mining and Metallurgy, Section A: Mining Technology*, vol. 110, pp. 27–39, https://doi.org/10.1179/mnt.2001.110.1.27

Reyes-Montes, J, Sainsbury, B, Pettitt, W, Pierce, M & Young, R 2016, 'Application of cave-scale rock degradation models in the imaging of the seismogenic zone', *CIM Journal*, vol. 7, https://doi.org/10.15834/cimj.2016.9

Rooz, A & Sainsbury, B 2026a, 'Mechanical degradation of granite under excavation-induced unloading: implications for design reliability', *Results in Engineering*, https://doi.org/10.1016/j.rineng.2026.110747

Rooz, A & Sainsbury, B 2026b, 'Geomechanical characterisation of intact Sydney sandstone (Class III) under loading and excavation-induced unloading', *Geomechanics for Energy and the Environment*, https://ssrn.com/abstract=6833558

Rooz, A & Sainsbury, B 2025a, 'Improving elastic parameter evaluation for hard brittle rock: a crack damage criterion based tangent 30 method', *Journal of Geotechnical Testing*, http://dx.doi.org/10.2139/ssrn.6540218

Rooz, A & Sainsbury, B 2025b, 'Adelaide black granite: geomechanical characterisation for underground design', *Australian Journal of Earth Sciences*, vol. 72, pp. 233–251, https://doi.org/10.1080/08120099.2025.2463604

Sainsbury, BL 2010, 'Sensitivities in the numerical assessment of cave propagation', in Y Potvin (ed.), *Caving 2010: Proceedings of the Second International Symposium on Block and Sublevel Caving*, Australian Centre for Geomechanics, Perth, pp. 523–535, https://doi.org/10.36487/ACG_rep/1002_36_Bsainsbury

Sainsbury, B 2012, *A Model for Cave Propagation and Subsidence Assessment in Jointed Rock Masses*, PhD thesis, University of New South Wales, Sydney, https://doi.org/10.26190/unsworks/16016

Sainsbury, B 2019, 'Consideration of the volumetric changes that accompany rock mass failure', *Rock Mechanics and Rock Engineering*, vol. 52, pp. 277–281, https://doi.org/10.1007/s00603-018-1560-8

Sainsbury, B, Pierce, ME & Mas Ivars, D 2008, 'Analysis of caving behaviour using a synthetic rock mass — ubiquitous joint rock mass modelling technique', in Y Potvin, J Carter, A Dyskin & R Jeffrey (eds), *SHIRMS 2008: Proceedings of the First Southern Hemisphere International Rock Mechanics Symposium*, Australian Centre for Geomechanics, Perth, pp. 243–253, https://doi.org/10.36487/ACG_repo/808_136

Sainsbury, B & Rooz, A 2025, 'A geological approach for the estimation of the confined elastic modulus of rock based on the Hoek-Brown mi constant', *Rock Mechanics and Rock Engineering*, https://doi.org/10.1007/s00603-025-05122-2

Sainsbury, B, Sainsbury, D & Carroll, D 2018, 'Back-analysis of PC1 cave propagation and subsidence behaviour at the Cadia East mine', in Y Potvin & J Jakubec (eds), *Caving 2018: Proceedings of the Fourth International Symposium on Block and Sublevel Caving*, Australian Centre for Geomechanics, Perth, pp. 167–178, https://doi.org/10.36487/ACG_rep/1815_10_Sainsbury

Sainsbury, D, Sainsbury, B, Paetzold, H-D, Lourens, P & Vakili, A 2016, 'Caving-induced subsidence behaviour of Lift 1 at the Palabora block cave mine', in *Seventh International Conference & Exhibition on Mass Mining*, AusIMM, Melbourne.

Snyman, L, Webster, S & Samosir, J 2016, 'E48 cave extension at Northparkes', in *Seventh International Conference & Exhibition on Mass Mining*, AusIMM, Melbourne, pp. 111–117.

Sougarret, J, Quinones, L, Morales, R & Apablaza, R 2004, 'New vision in caving mining in Andina Division, Codelco Chile', in *MassMin 2004*, Santiago, pp. 542–546.

Stegman, C, van As, A & Peebles, E 2018, 'Past learnings focus innovative solutions to future cave mining', in Y Potvin & J Jakubec (eds), *Caving 2018: Proceedings of the Fourth International Symposium on Block and Sublevel Caving*, Australian Centre for Geomechanics, Perth, pp. 37–42, https://doi.org/10.36487/ACG_rep/1815_0.3_Stegman

Tyler, DB & Godden, SJ 2008, 'Geotechnical Modelling for Kimberlite Pipes', in Y Potvin, J Carter, A Dyskin & R Jeffrey (eds), *SHIRMS 2008: Proceedings of the First Southern Hemisphere International Rock Mechanics Symposium*, Australian Centre for Geomechanics, Perth, pp. 551–564, https://doi.org/10.36487/ACG_repo/808_159

Van As, A & Jeffrey, R 2000, 'Caving induced by hydraulic fracturing at Northparkes Mines', in Girard, Liebman, Breeds & Doe (eds), *Proceedings of the 4th North American Rock Mechanics Symposium*, Balkema, Seattle, pp. 353–360.

Woo, KS, Eberhardt, E, Rabus, B, Stead, D & Vyazmensky, A 2012, 'Integration of field characterisation, mine production and InSAR monitoring data to constrain and calibrate 3-D numerical modelling of block caving-induced subsidence', *International Journal of Rock Mechanics and Mining Sciences*, https://doi.org/10.1016/j.ijrmms.2012.05.008